ECORFAN-Journal Taiwan 8[15]1-12: e2815112
Article

Thermoeconomic analysis in solar collector fields: a focus on constant flowrate and variable flowrate models

Análisis termoeconómico en campos de colectores solares: un enfoque en los modelos de flujo constante y flujo variable

Lugo-Granados, Hebert Gerardo*[a], Canizalez-Dávalos, Lázaro[b] and Picón-Núñez, Martín[c]

[a] Autonomous University of Zacatecas • F-2050-2019 • 0000-0002-0027-3418 • 487049
[b] Autonomous University of Zacatecas • ABW-3215-2022 • 0000-0002-3126-8574 • 164509
[c] University of Guanajuato • AHA-5481-2022 • 0000-0002-0793-192X • 12408

CONAHCYT classification:

Area: Engineering
Field: Engineering
Discipline: Mechanical Engineering
Subdiscipline: Energy

https://doi.org/10.35429/EJT.2024.8.15.1.12
History of the article:
Received: February 25, 2024
Accepted: December 19, 2024

* ✉ [lugh871024@gmail.com]

Abstract

In this study, the operation models with constant flowrate and variable flowrate of a flat-plate solar collector field are analysed. The model that achieves greater energy utilization and lower operating costs was determined under two conditions: when scaling fouling occurs in the collector tubes and when a clean operation (without fouling) is considered. The case study involves a pasteurization plant operating at temperatures above 85°C. The operational scenarios are as follows: 1) Variable flowrate: the flowrate is adjusted based on environmental conditions to maintain a constant outlet temperature, and 2) Constant flowrate: the flowrate remains constant, resulting in varying collector outlet temperatures depending on weather conditions. The results show that under clean conditions, operating with variable flowrate yields a lower cost per kWh of captured energy ($0.048/kWh). In the presence of fouling, the cost of operating with variable flowrate significantly increases to $0.15/kWh, while constant flowrate results in the lowest cost ($0.077/kWh).

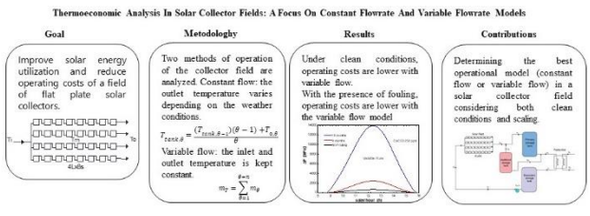

Collectors, Networks, Scaling

Resumen

En el presente trabajo se analizan los modelos de operación con flujo constante y flujo variable de un campo de colectores solares de placa plana. Se determinó el modelo que presenta mayor aprovechamiento de energía y menores costos de operación en dos condiciones, cuando se tiene ensuciamiento por scaling en los tubos del colector y cuando se considera una operación limpia (sin ensuciamiento). El caso de estudio es una planta pasteurizadora que opera a temperaturas mayores a 85°C. Los escenarios de operación son: 1) Flujo variable: el flujo se modifica en función de las condiciones ambientales para mantener la temperatura de salida constante y 2) Flujo constante: se mantiene constante el flujo, por lo que la temperatura a la salida de los colectores varía en función de las condiciones climatológicas. Los resultados muestran que en condiciones limpias al operar con flujo variable se obtiene un menor costo por kWh de energía capturada (0.048$/kWh). En presencia de ensuciamiento el costo de operar con flujo variable aumenta considerablemente a 0.15$/kWh, mientras que con flujo variable se obtiene el menor costo (0.077 $/kWh).

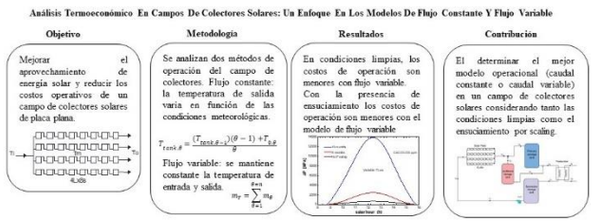

Colectores, Redes, Scaling.

Citation: Lugo-Granados, Hebert Gerardo, Canizalez-Dávalos, Lázaro and Picón-Núñez, Martín. [2024]. Thermoeconomic analysis in solar collector fields: a focus on constant flowrate and variable flowrate models. ECORFAN-Journal Taiwan. 8 [15]1-12: e2815112.

Introduction

In this work, we aim to understand the operating model (constant flowrate or variable flowrate) of a solar collector field that achieves optimal thermal performance and lower operating costs.

Operating with a constant flowrate model allows leads to higher temperatures than required by the process, resulting in excess thermal load. On the other hand, operating with variable flowrate leads to attain more hot water than necessary, also leading to excess thermal load. Increasing the water flowrate through the collectors results in additional pressure drops and consequently raises operating costs.

The excess thermal load obtained can be stored for use when there is a solar energy deficit or to increase production.

When designing a solar collector network, it is necessary to consider the climatic variations that occur during a typical solar day, such as air velocity, solar radiation, ambient temperature, etc. However, the design should always prioritize energy utilization and minimize energy losses. In the case of the pasteurization process, it is challenging to avoid energy losses because the collector inlet temperatures must exceed 75°C (Hanson et al., 2005). This condition requires high solar radiation (<550W/m²) to produce thermal energy at these temperatures.

Weather conditions, for example: poor solar radiation, low ambient temperatures, and high air velocities, as well as scaling fouling, are parameters that directly affect the thermal and hydraulic performance of solar collectors (Bunea et al., 2012). Over time, scaling fouling also causes thermal and hydraulic problems by depositing mineral salts (CaCO3) inside the tubes.

Operating variables (volumetric flowrate rate, inlet temperature, and operating time) are parameters that can be modified to improve the performance of solar collectors. When the radiation level is lower than that used for network design, the outlet temperature of the collectors is lower than the inlet temperature, resulting in thermal energy loss. To prevent energy losses when radiation decreases, the flowrate velocity can be adjusted based on weather conditions.

Various authors have reported works where they have analysed the influence of operating variables and climatic conditions on the thermal performance of solar collectors. Dembeck-Kerekes et al. (2019) introduced a strategy for variable flowrate control in a thermal-photovoltaic collector to optimise energy generation. Sokhansefat et al.

(2018) found that inlet temperature and climatic conditions are the main variables affecting the performance of a solar collector when operating in cold weather. Climatic conditions significantly impact solar energy utilization. Zhuang et al. (2024) determined that radiation has a greater impact compared to other parameters. However, all climatic conditions must be considered to ensure robust designs, analyses, and results.

There are studies focused on developing models to determine the performance of a flat plate solar collector considering the effects of solar radiation, mass flow rate, and the geometric parameters. Majumdar et al. (2020) conducted research in this area. Unterberger et al. (2021) and Momodu-Bangura et al. (2022) determined the performance of a flat plate collector and a double-pass solar collector through the cover, respectively, by varying solar radiation and ambient temperature. Du et al. (2022) presented a method that combines input data such as solar radiation, ambient temperature, air velocity, fluid flow rate, and fluid inlet temperature with an artificial neural network model to improve the accuracy of vacuum tube solar collectors' performance. Wang et al. (2021) proposed a numerical model to analyse the effects of network configuration, flowrate, inlet temperature, and working fluid on pressure drops and outlet temperatures in a field of flat plate solar collectors.

Studies reported so far, do not consider scaling fouling in their models or experimental results. In the literature, there are few studies that include scaling fouling in the operation of solar collectors. Arunachala et al. (2015) provided an overview of the effects caused by radiation and scaling fouling on the instantaneous efficiency variation of a solar collector. Lugo-Granados et al. (2023) investigated the effects of scaling fouling on the thermohydraulic performance of a network of solar collectors.

ISSN: 2524-2121.
RENIECYT-CONAHCYT: 1702902

Lugo-Granados, Hebert Gerardo, Canizalez-Dávalos, Lázaro and Picón-Núñez, Martín. [2024]. Thermoeconomic analysis in solar collector fields: a focus on constant flowrate and variable flowrate models. ECORFAN-Journal Taiwan. 8 [15]1-12: e2815112.
https://doi.org/10.35429/EJT.2024.8.15.1.12

In 2024, Lugo-Granados et al. determined the optimal network design for a field of solar collectors in terms of operational costs and thermal load acquisition, both under clean conditions and when scaling fouling is present.

These studies maintain constant operating parameters such as volumetric flow rate and climatic conditions (ambient temperature and air velocity). Variations in these parameters can mitigate the effects caused by scaling fouling and enhance the performance of the solar collector network.

The contribution of this research consists of determining the best operational model within two scenarios: constant flowrate and variable flowrate in a field of flat plate solar collectors to provide thermal load to a pasteurization plant. Additionally, the goal is to identify the model that enhances solar energy utilization and results in the lowest operating costs, considering both clean conditions and scaling fouling.

Case study: Pasteurization plant

The case study involves a thermosolar plant responsible for supplying thermal load to a milk pasteurization process (2010). A total of 3,500 liters of milk are pasteurized daily. The entire amount of water heated during the day is used to perform pasteurization at 7:00 a.m. the following day.

Figure 1 shows the operational diagram of the pasteurization plant. The installation consists of a primary circuit composed of the solar collector field and storage tanks, which connect to the secondary thermal treatment circuit. The secondary circuit has three stages: pasteurization, recovery, and cooling. Hot water obtained from the solar collector field is stored in the primary container at 82°C. It then passes through the pasteurizer exchanger, where its temperature drops to 76°C. Finally, it is stored in the secondary container to circulate back through the collectors.

Meanwhile, the milk enters the pasteurizer at a temperature of 72°C and exits at 80°C. The hot water leaving the solar collectors must have a temperature higher than 82°C to ensure pasteurization.

During the pasteurization process, the milk temperature must be raised to 72-75°C and maintained at the same temperature for 15 to 20 seconds. In the recovery and heat-saving stage, cold (unpasteurized) milk is preheated with the hot outlet milk (pasteurized).

In the cooling stage, the milk temperature is reduced below 4°C.

Box 1

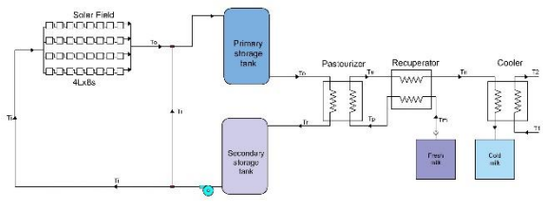

Figure 1
Pasteurization plant diagram

The solar field consists of 32 collectors divided into 4 rows, each with 8 collectors connected in series (4Lx8s), where the letters 'L,' 'p,' and 's' indicate line, parallel, and series, respectively (Figure 2). The number of collectors in series ensures that around 30% of the solar hours in a year, the water temperature at the outlet of the last collector in series will be above 80°C.

The working period for the solar collectors is 8 hours, from 8:00 in the morning until 16:00 in the afternoon. The total water flowrate passing through the collector network is 401.12 liters per hour, resulting in a daily storage of 3,209 liters of hot water. The water flowrate required to pasteurize 3,500 liters of milk within an hour must be equal to or greater than this amount for effective heat exchange.

In the Table 1 shows main features of flat plate solar collectors.

Box 2

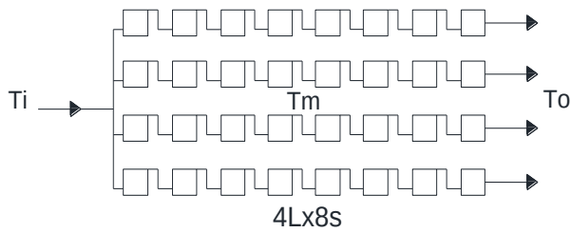

Figure 2
Configuration of the solar collector network

ISSN: 2524-2121.
RENIECYT-CONAHCYT: 1702902

Lugo-Granados, Hebert Gerardo, Canizalez-Dávalos, Lázaro and Picón-Núñez, Martín. [2024]. Thermoeconomic analysis in solar collector fields: a focus on constant flowrate and variable flowrate models. ECORFAN-Journal Taiwan. 8 [15]1-12: e2815112.
https://doi.org/10.35429/EJT.2024.8.15.1.12

Box3

Table 1

Main geometrical features of flat plate solar collectors

Dimensions	**Length**	**width**	**Absorber / Total area**
	2,190 (mm)	1,090 (mm)	2.13 (m^2) / 2.40 (m^2)
Absorber tube	**Number of tubes**	**External diameter**	**Internal diameter**
	10	10 (mm)	8 (mm)
Cover	**Material**	**Transmittance**	**Thickness**
	Tempered solar glass	0.91	3.20 (mm)
Absorber	**surface absorptivity**	**Thickness**	**Surface Emissivity**
	0.95	0.4 (mm)	0.05
Tubes collectors	**Number of tubes**	**External diameter**	**Internal diameter**
	2	22 (mm)	20 (mm)
Insulating and shell	**Bottom insulation thickness**	**Side insulation thickness**	**Material**
	30 (mm)	30 (mm)	Polyurethane + mineral wool

Methodology

Operation modes: Constant flowrate and variable flowrate

The operation of the solar collector field is a continuous process. The secondary tank feeds the solar field during the day at a constant inlet temperature, Ti (°C). The useful heat quantity, Qu (kW), obtained from the collectors can be determined from Eqs. 1 to 7.

$$Q_{u,\theta} = \dot{m}_{f,\theta}\, C_{p,\theta}(T_{0,\theta} - T_{i,\theta}) \quad (1)$$

$$Q_{u,\theta} = F_{R,\theta} A_{s,\theta}\left[I_{G,\theta}(\tau\alpha_c) - U_{c,\theta}\left(T_{pm,\theta} - T_{a,\theta}\right)\right] \quad (2)$$

Where Θ is the cycle iteration, As (m^2) is the plate surface area, $\dot{m}_f$ (kg/s) is the mass flowrate, C_p (kJ/Kg°C) is the specific heat, T_i and T_0 (°C) are the inlet and outlet temperature in the tubes respectively. (F_R) is the heat removal factor from the plate to the fluid, T_{pm} (°C) is the temperature of the plate and T_a (°C) is the ambient temperature (°C), (α_c y τ) are the absorbance and transmittance of the transparent cover and the term I_G (W/m^2) is the solar radiation intensity.

In Eq. (3), the heat removal factor FR is presented, which depends on the overall heat transfer coefficient Uc (W/m²°C) and the collector efficiency factor F' (Eq. 4).

$$(4))\ F_{R,\theta} = \frac{\dot{m_{f,\theta}} C_{P,\theta}}{A_S\, U_{c,\theta}}\left[1 - e^{\frac{-A_S\, U_{c,\theta} F_\theta^{'}}{\dot{m}_f C_{P,\theta}}}\right] \quad (3)$$

The collector efficiency factor primarily depends on the resistance to heat transfer from the absorber plate to the working fluid. These resistances manifest through the junction between the plate and the tube, denoted as C_b (m² °C/W) in Eq. (5). They arise due to the tube wall (Rt, m² °C/W), fouling layer (Rs, m² °C/W), and the convection resistance between the tube's inner wall and the working fluid (Rh, m² °C/W). Additionally, it is influenced by the fin efficiency (FA), expressed in Eq. (6).

$$F_\theta^{'} = \frac{1/U_{c,\theta}}{S\left[\frac{1}{U_{c,\theta}\left[d_0 + F_{A,\theta}(S-d_0)\right]} + \frac{1}{C_{b,\theta}} + \frac{R_{h,\theta}}{\pi d_{s,\theta}} + \frac{R_{t,\theta}}{\pi d_{s,\theta}} + \frac{R_{s,\theta}}{\pi d_{s,\theta}}\right]} \quad (4)$$

$$C_{b,\theta} = \frac{k_{b,\theta} W}{\gamma} \quad (5)$$

Where k_b represents thermal conductivity, W (m) is the width of the junction, and γ (m) is the thickness of the junction between the plate and the tube. d_i and d_0 (m) denote the inner and outer diameters, S (m) is the distance between tubes.

$$F_{A,\theta} = \frac{Tanh[M(S-d_0)/2]}{M_\theta(S-d_0)/2} \quad (6)$$

While M (m^{-1}) is expressed in Eq.(7), where K_s (W/m°C) and δ (m) are the thermal conductivity and the plate thickness.

$$M_\theta = \sqrt{\frac{U_{c,\theta}}{K_s \delta}} \quad (7)$$

The instantaneous efficiency (η) of the collectors is determined from Eq.(8).

$$\eta_\theta = \frac{Q_{u,\theta}}{I_{G,\theta} A_s} \quad (8)$$

The total heat load Q_T (kW) stored in the tank is the sum of the thermal load per cycle, Eq.(9).

$$Q_T = Qu,1 + Qu,2 + Qu,3 + \cdots + Qu,n \quad (9)$$

ISSN: 2524-2121.
RENIECYT-CONAHCYT: 1702902

Lugo-Granados, Hebert Gerardo, Canizalez-Dávalos, Lázaro and Picón-Núñez, Martín. [2024]. Thermoeconomic analysis in solar collector fields: a focus on constant flowrate and variable flowrate models. ECORFAN-Journal Taiwan. 8 [15]1-12: e2815112.
https://doi.org/10.35429/EJT.2024.8.15.1.12

A mathematical model developed by Lugo-Granados et al. (2018) was implemented to determine the amount of scaling (CaCO3) deposited in the tubes of solar collectors. Eq. 10 describes this process.

$$\dot{m}_{d,\theta} = \frac{\beta}{2}\left(\frac{\beta,\theta}{\alpha\, k_{r,\theta}} + (C_1 + C_2) - \sqrt{\frac{[\beta,\theta + (C_{1+}C_2)\,\alpha,\theta\, k_{r,\theta}]^2 + 4\,\alpha_\theta^2\, k_{r,\theta}{}^2 (K_{sp,\theta} - [C_1][C_2])}{\alpha_\theta^2\, k_{r,\theta}{}^2}}\right) \quad (10)$$

The model calculates the mass flux $\dot{m}_d$ (kg/m^2 s) of $CaCO_3$ deposited inside the tubes, considering parameters involved in scaling formation such as pH, the concentration of Ca_2+ (C1) (kg/m^3), CO_3^{2-} (C2) (kg/m^3), and the solubility Ksp (kg^2/m^6) of CaO_3 in water.

The model also incorporates the chemical reaction constant k_r (m^2/kg s), which describes the rate of crystal formation. Another variable is the mass transfer coefficient β (m/s). Additionally, the dimensionless deposition resistance factor α (Eq. 10) accounts for viscous and inertial effects affecting crystal deposition on the surface. Over time, fouling increases, leading to changes in tube roughness and diameter, resulting in greater pressure drop.

$$\alpha_\theta = \frac{191}{f \cdot Re^{1.67}} \quad (10)$$

The calculation of the mass flux, $\dot{m}_d$ (kg/m² s), deposited allows determining the thermal resistance generated by fouling during the operation of solar collectors using Eq. (11). According to this expression, the thermal resistance due to fouling, Rs (m² °C/W), is also a function of the mass flux that is removed, $\dot{m}_r$ (kg/m² s), Quan, et al. (2008); the density ρ_f (kg/m³) and the thermal conductivity λ_f (W/m °C) of $CaCO_3$.

$$\frac{dR_{s,\theta}}{dt,\theta} = \frac{\dot{m}_d - \dot{m}_r}{\rho_f \lambda_f} \quad (11)$$

When operating with the constant flowrate model, the outlet temperature varies in each cycle based on climatic conditions and the presence of scaling fouling. Therefore, the obtained useful load Q_u (kW) depends solely on the outlet temperature, T_0 (°C).

The temperature reached by the water in the storage tank ($T_{tank,\Theta}$) results from the mixture of water leaving the collectors in each cycle ($T_{0,\Theta}$) and the tank temperature obtained in the previous cycle ($T_{tank,\Theta-1}$), Eq. (12).

$$T_{tank,\theta} = \frac{(T_{tank,\theta-1})(\theta-1)+T_{0,\theta}}{\theta} \quad (12)$$

For the variable flowrate model, the amount of water $\dot{m}_f$ (kg) passing through the solar collector field varies based on environmental conditions and scaling fouling to maintain a constant outlet temperature T_o (in °C).

Therefore, the useful heat (Q_u (kW)) obtained from the collectors depends solely on the water flowrate, as described by Equation 1. The mass deposited in the storage tank during each cycle *m* (kg) depends on the mass flow rate $\dot{m}_f$ (kg/s) in each cycle and the cycle time, t (s) as given by Eq.13.

$$m_{,\theta} = \dot{m}_{f,\theta} \cdot t_\theta \quad (13)$$

The total mass m_T (kg) is the summation of each cycle, Eq. (14). The mass excess is storage in an additional tank (Figure 3).

$$m_T = \sum_{\theta=1}^{\theta=n} m_\theta \quad (14)$$

For the variable flowrate model, pressure drop varies in each cycle. Starting from Eq. (15), we obtain the pressure drop within the collector network, which is proportional to the sum of hydraulic resistances K_i (kPa s²/m⁶) and the square of the volumetric flow rate $\dot{V}$ (m³/s).

$$\Delta P_{T,\theta} = \dot{V}_\theta^2 \sum_{i=1}^{n} K_i \quad (15)$$

Eqs. (16 and 17) show the main hydraulic resistances. The resistance generated by friction, denoted as K_1 (kPa s²/m⁶), is due to the pipe length. Additionally, the resistance generated by accessories, represented by K_2 (kPa s²/m⁶), such as elbows, valves, and unions, is considered.

$$K_{1,\theta} = \frac{8L_t}{\pi^2 (d_{s,\theta})^5} f_\theta \quad (16)$$

$$K_{2,\theta} = \frac{8\rho}{\pi^2 (d_{s,\theta})^5} k_f \quad (17)$$

ISSN: 2524-2121.
RENIECYT-CONAHCYT: 1702902

Lugo-Granados, Hebert Gerardo, Canizalez-Dávalos, Lázaro and Picón-Núñez, Martín. [2024]. Thermoeconomic analysis in solar collector fields: a focus on constant flowrate and variable flowrate models. ECORFAN-Journal Taiwan. 8 [15]1-12: e2815112.
https://doi.org/10.35429/EJT.2024.8.15.1.12

where f is the friction factor along the pipe, k_f, is the resistance factor for each accessory, L_t (m) and d_s (m) are the length and hydraulic diameter of the tube. It is observed that reducing the diameter increases flow resistance, leading to higher pressure drop.

Box 4

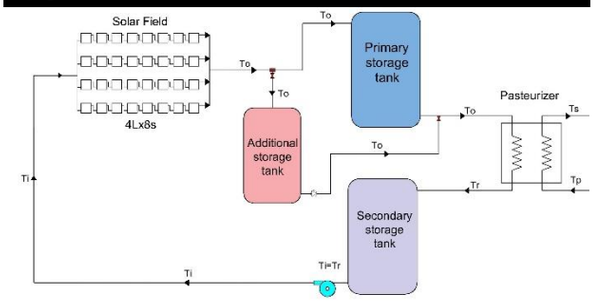

Figure 3

Primary circuit of the pasteurizer plant with energy storage

Cost Model

The total operating cost $Cost_{total}$ ($) is the sum of pumping costs per cycle and the annualized cost of collectors, Eq. (18).

$$Cost_{total} = Cost_b + Cost_a \quad (18)$$

The pump operating cost $Cost_b$ ($) is directly proportional to pump power, operation time t (h), and the unit cost of electricity Costu ($/kWh). Eq. (19) assumes an electricity cost of $0.3/kWh.

$$Cost_{b,\theta} = cost_u \dot{w}_\theta \, t \quad (19)$$

Pump power depends on volumetric flow rate $\dot{V}$ (m^3/s), pump pressure drop ΔP (kPa), and pump efficiency (ηb), Eq.(20).

$$\dot{w}_\theta = \frac{\dot{V}_\theta \Delta P_\theta}{\eta_b} \quad (20)$$

The Annualised Cost of Collectors ($Cost_a$) is equal to the cost per collector Cu ($) multiplied by the annualization factor Ƒa and the total number of collectors ((Nc)), Eq.(21). The estimated commercial cost per collector is $811.76 USD. To calculate the annualization factor ((Ƒa)), we consider a collector lifespan (ω) of 20 years and an annual interest rate ï of 8%. Eq.(22).

$$Cost_a = C_u \cdot Fac_A \cdot N_c \quad (21)$$

$$Ƒ_a = \left[\frac{ï(1+ï)^\omega}{(1+ï)^\omega - 1}\right] \quad (22)$$

Results

Climate Conditions

Graph 1 depicts ambient temperature and air velocity throughout a typical spring day in central Mexico. The minimum ambient temperature is 17°C, and the maximum is 32°C. Air velocity varies from 2.2 m/s to 10 m/s.

Graph 2 illustrates solar radiation over the course of the day, reaching a peak value of 1,106 W/m² at 12:45 h.

Box 5

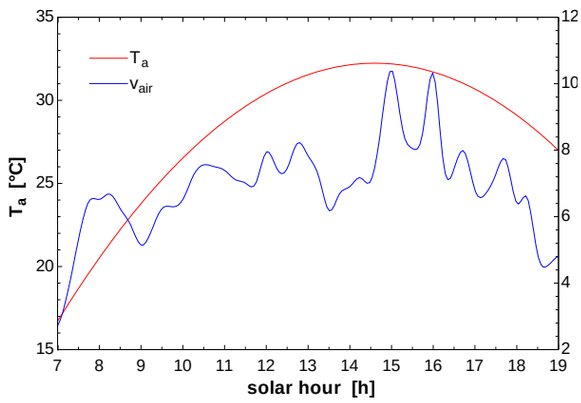

Graph 1

Typical variation of ambient temperature and wind velocity with solar time (Central Mexico)

Box 6

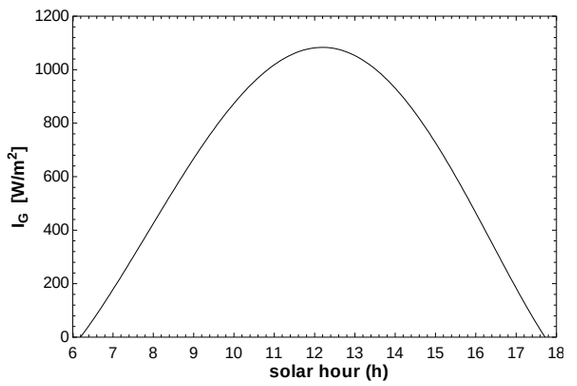

Graph 2

Solar radiation with respect to solar time.

Graph 3 presents graphs of the outlet temperature from a collector field relative to ambient temperature for different air velocities.

ISSN: 2524-2121.
RENIECYT-CONAHCYT: 1702902

Lugo-Granados, Hebert Gerardo, Canizalez-Dávalos, Lázaro and Picón-Núñez, Martín. [2024]. Thermoeconomic analysis in solar collector fields: a focus on constant flowrate and variable flowrate models. ECORFAN-Journal Taiwan. 8 [15]1-12: e2815112.
https://doi.org/10.35429/EJT.2024.8.15.1.12

The inlet temperature, volumetric flow rate, and solar radiation remain constant. Under these conditions, a 10°C increase in ambient temperature leads to a 1°C rise in outlet temperature across various air velocities. Additionally, increasing air velocity from 6 m/s to 10 m/s reduces the outlet temperature by 0.3°C.

Graph 4 shows that a 1 m/s increase in air velocity the solar collector's outlet temperature decreases by 0.1°C.

Box 7

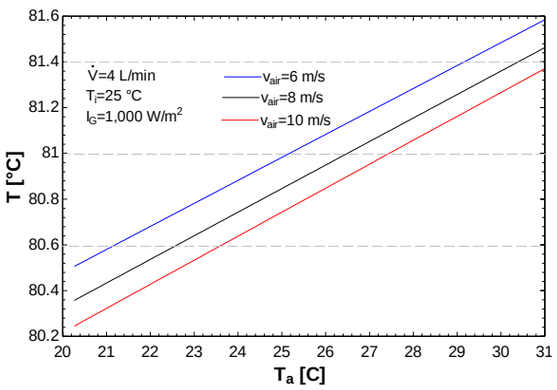

Graph 3

Fluid outlet temperature for different fluid mass flow rate

Box 8

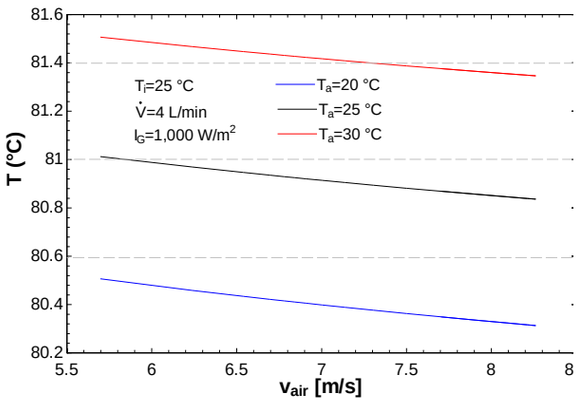

Graph 4

Fluid outlet temperatura with respect to air velocity for differnt ambient temperature

Network design

An analysis was conducted to determine the appropriate network design for raising the temperature from 75°C to 85°C with a total volumetric flow rate of 6.685 L/min. The network design involves determining the number of collectors per line connected in series to achieve the target temperature. The network should consist of 4 lines to provide the necessary thermal load.

From the obtained results (Graph 5), it is found that to reach the target temperature (85°C), operation is required with radiation greater than 550 W/m², as under these conditions, the maximum temperature reached is 84.5°C with 51 collectors in series per line. When there is a radiation of 575 W/m², 17 collectors per line are needed to reach the target temperature. Increasing radiation reduces the required number of collectors to achieve the target temperature.

With radiation of 625 W/m², 8 collectors are needed to achieve a temperature of 85°C, representing a 53% reduction in area compared to designing with radiation of 575 W/m² (17 collectors). Consequently, the start time for operating the collector network should be delayed by approximately 15 minutes to obtain a radiation of 625 W/m² (see Figure 5).

On the other hand, having a solar field with 17 collectors per line results in greater energy gain but also higher costs. According to Lugo-Granados et al. [XI], Rs-p represents the ratio between the number of lines (N_L) and parallel collectors (Np) to the quantity of series collectors (N_p). A value of R_{s-p} closer to 1 indicates better performance of the network from a thermohydraulic and economic perspective. When there are 8 collectors per line, the R_{s-p} value is 2, whereas with 17 collectors per line, R_{s-p} = 4.25. Based on this, the network design with 8 collectors is superior.

$$R_{s-p}^{-1} = \frac{N_L \cdot N_p}{N_s} \tag{23}$$

Box 9

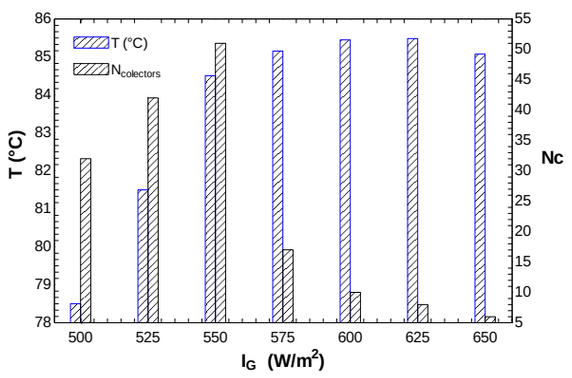

Graph 5

Number of solar collectors in series to reach the objective temperature with respect to solar radiation. T_i=75°C, volumetric flow rate=6.685 l/min.

ISSN: 2524-2121.
RENIECYT-CONAHCYT: 1702902

Lugo-Granados, Hebert Gerardo, Canizalez-Dávalos, Lázaro and Picón-Núñez, Martín. [2024]. Thermoeconomic analysis in solar collector fields: a focus on constant flowrate and variable flowrate models. ECORFAN-Journal Taiwan. 8 [15]1-12: e2815112.
https://doi.org/10.35429/EJT.2024.8.15.1.12

Effect of scaling fouling in the operation models: constant flowrate and variable flowrate

In Graph 6, graphs of the volumetric flow rate necessary to maintain a constant outlet temperature (85°C) are shown with respect to solar time. Environmental conditions change throughout the day, so the flowrate must be adjusted to maintain a constant outlet temperature. As solar time increases, the amount of energy received by the collectors also increases, necessitating flowrate adjustments to maintain the desired outlet temperature, reaching a maximum when solar radiation is highest (see Figure 4).

Under clean conditions (black line, Graph 6), higher flow rates are achieved, resulting in greater thermal load. Over time, the presence of scaling fouling on the collectors (blue and red lines, Graph 2) increases, causing a reduction in the amount of solar energy absorbed. Therefore, volumetric flow rates must be reduced relative to when there is no fouling to maintain the constant outlet temperature.

Box 10

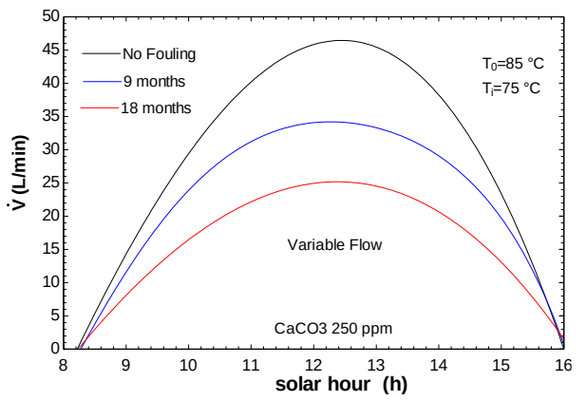

Graph 6

Variation of volumetric flow rate with the day

When operating with variable flowrate, pressure drop varies throughout the solar day (Graph 7).

In the presence of scaling fouling (blue and red lines, Graph 7), pressure drops increase significantly after 18 months of operation due to deposits on the collectors increasing hydraulic resistance.

Box 11

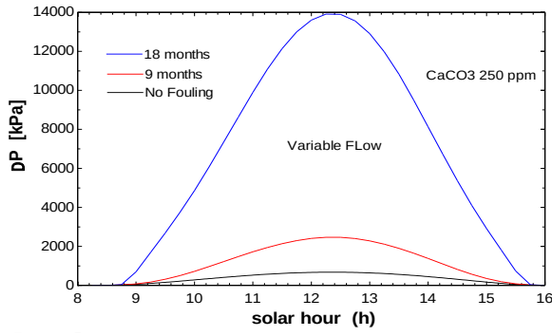

Graph 7

Pressure drop variation during the day for fouling established at different accumulated operation times compared to clean conditions

When operating with constant flowrate, the outlet temperature of solar collectors varies throughout a solar day (see Graph 8). As solar time changes, the outlet temperature in the solar field also adjusts. The highest temperature is obtained at noon when solar radiation is at its maximum. Under clean conditions (black line, Graph 8), a maximum temperature of 114.5°C is reached. After 9 months of operation, the maximum achievable temperature decreases to 113.5°C. When operating for 18 months, the maximum temperature achieved is 112°C.

Box 12

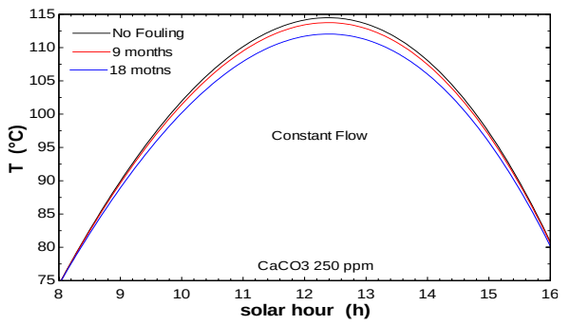

Graph 8

Outlet temperature vs solar time for different volumetric flow rates

In Graph 9, graphs of the thermal load generated by the collectors are shown with respect to solar time when fouling is present for both constant flowrate and variable flowrate models. With the variable flowrate model under clean conditions, the highest instantaneous thermal load is obtained (2,900 kWh). After operating for 9 months, the energy level achieved is 2,100 kWh. At 18 months, the maximum is 1,550 kWh, representing a 46.5% reduction compared to clean conditions.

ISSN: 2524-2121.
RENIECYT-CONAHCYT: 1702902

Lugo-Granados, Hebert Gerardo, Canizalez-Dávalos, Lázaro and Picón-Núñez, Martín. [2024]. Thermoeconomic analysis in solar collector fields: a focus on constant flowrate and variable flowrate models. ECORFAN-Journal Taiwan. 8 [15]1-12: e2815112.
https://doi.org/10.35429/EJT.2024.8.15.1.12

Box 13

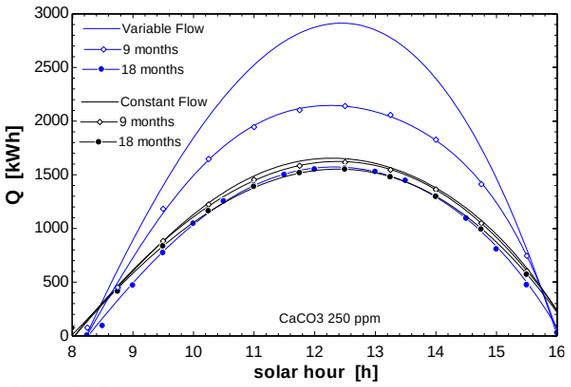

Graph 9

Heat load with respect to solar time for the two models considering fouling

For the constant flowrate model, the maximum instantaneous energy obtained is 1,650 kWh when no fouling is present. After 18 months of operation, the thermal load decreases by 1,000 kWh, representing a 6.5% reduction. These results indicate that scaling fouling has a greater effect on the variable flowrate model.

Cost Analysis

In Tables 2 to 4, the results of the annualised cost analysis for constant flowrate and variable flowrate models are presented under clean conditions and when scaling occurs. The reference case indicates the minimum operating variables required for the process. The flowrate of 6,685 l/min takes 15 minutes to flow through the entire network. Therefore, the analysis was conducted within this time interval.

The inlet temperature is maintained at 75°C. The thermal load and operating costs obtained in each interval are summed to obtain the total. The annualized cost for the 32 collectors is $2,597.65, and this value is added to the pumping cost to obtain the total cost.

The unit cost is obtained by dividing the total cost by the total thermal load.

From the results, it is observed that operating with the variable flowrate model (Table 2) generates the lowest unit cost (0.048 /kWh). The obtained thermal load (59,613.12kWh) exceeds the reference case load by331/kWh. Compared to the reference case, costs are reduced by 61.9%, and 162% more thermal load is produced.

When comparing solar energy usage with natural gas, which has an international price of 0.1 $/kWh, it is found that solar energy has a lower cost.

However, the scaling fouling effect on the collectors must be considered, as their thermohydraulic performance significantly decreases after a period of operation.

Box 14

Table 2

Cost analysis for different modes of operation without fouling

Flowrate (l/min)	ΔP (kPa)	Cost_pump ($)	Cost Total ($)	Q (kWh)	Cost_Q ($/kWh)	T_o (°C)	T_tank (°C)
Reference case							
6.685	14.66	16.08	2,613.72	13,831.93	0.189	85	85
Constant flowrate							
6.685	14.66	16.08	2,613.72	36,239.59	0.072	Variable	101.20
Variable flowrate							
Variable	Variable	297.33	2,894.98	59,613.12	0.048	85	85

After 9 months of operation, considering the presence of scaling-induced fouling (Table 3), using the constant flowrate model results in a temperature drop of 0.5°C in the storage tank.

The thermal load produced decreases by 1.9%, and the unit price increases by 2% compared to when no fouling exists. For the variable flowrate model, the thermal load is reduced by 22%, while the unit cost increases by 44%.

Box 15

Table 3

Cost analysis for different operation modes with fouling (9 months operation)

Flowrate (l/min)	ΔP (kPa)	Cost_pump ($)	Cost Total ($)	Q (kWh)	Cost_Q ($/kWh)	T_o (°C)	T_tank (°C)
Reference case							
6.685	19.56	16.64	2,614.30	13,728.00	0.19	85	85
Constant flowrate							
6.685	Variable	16.62	2,614.26	35,560.89	0.0735	Variable	100.7
Variable flowrate							
Variable	Variable	634.33	3,231.98	46,357.83	0.0697	85	85

When operating with the variable flowrate model for 18 months, from a thermal perspective, it remains profitable, but not economically viable, as the cost increases to 0.154 kWh, which is no longer competitive compared to natural gas usage (0.1 $/kWh). When operating for 18 months with the constant flowrate model, considering scaling presence, the temperature in the storage tank drops by 1.7°C, the thermal load decreases by 6%, and the unit cost increases by 7% compared to clean conditions.

ISSN: 2524-2121.
RENIECYT-CONAHCYT: 1702902

Lugo-Granados, Hebert Gerardo, Canizalez-Dávalos, Lázaro and Picón-Núñez, Martín. [2024]. Thermoeconomic analysis in solar collector fields: a focus on constant flowrate and variable flowrate models. ECORFAN-Journal Taiwan. 8 [15]1-12: e2815112.
https://doi.org/10.35429/EJT.2024.8.15.1.12

Despite this, it remains economically viable in terms of thermal load, although regular cleaning maintenance is necessary.

Box 16

Table 4

Cost analysis for different operation modes with fouling (18 months operation)

Flowrate (l/min)	ΔP (kPa)	Cost_pump ($)	Cost Total ($)	Q (kWh)	Cost_Q ($/kWh)	T_o (°C)	T_tank (°C)
Reference case							
6.685	36.88	$18.67	$2,616.32	13,662.000	$0.191	85	85
Constant flow rate							
6.685	Variable	18.56	2,616.21	33,904.90	0.077	Variable	99.5
Variable flowrate							
Variable	Variable	2,503.64	5,101.29	32,979.48	0.154	85	85

Conclusions

The solar collector's inlet temperature is relatively high at 75°C, requiring elevated radiation (<550 W/m²) to reach the target temperature. With radiation below 600 W/m², 17 collectors are needed to achieve the target temperature (85°C).

Operating above this radiation level reduces the required area by 53%.

Therefore, it is recommended to operate during hours when radiation exceeds 600 W/m² rather than attempting to increase the collection area. However, there is no specific operating schedule for the network.

According to the network design, a configuration of 4 lines with 8 series-connected heat exchangers per line is sufficient to provide the thermal load to the process. It exhibits good thermohydraulic performance according to the series-parallel relationship (Rs-p=2). However, operation should begin when radiation exceeds 600 W/m². With this network configuration, operating with constant flowrate can increase the required thermal load (13,831.93 kWh) by 162% (36,239.59 kWh), while variable flowrate increases it by 331% (59,613.12 kWh).

Under clean conditions, operating with variable flowrate presents better thermoeconomic performance compared to constant flowrate. Without fouling, the variable flowrate model achieves a 64% higher thermal load and 33% lower unit operating costs than the constant flowrate model.

Using solar collectors with a variable flowrate model for pasteurization reduces costs by more than half (0.048 /kWh) compared to natural gas usage (assuming a unit cost of 0.1/kWh). However, the effects of scaling fouling on solar collectors must be considered. If operated without maintenance for 18 months, the cost increases to 0.154 $/kWh.

In the presence of scaling, it is better to operate with constant flowrate since fouling has a lesser impact on the thermoeconomic performance of the collectors. If maximising solar field benefits, operating with constant flowrate and performing cleaning at least once a year is ideal for economic viability.

Declarations

Conflict of interest

The authors declare no interest conflict. They have no known competing financial interests or personal relationships that could have appeared to influence the article reported in this article.

Author contribution

Lugo-Granados, Hebert Gerardo: Contributed to the research methodology and generation of results and writing of the manuscript.

Canizalez-Dávalos, Lázaro: Contributed to the research method and revision of the manuscript.

Picón-Núñez, Martín: Contributed to the project idea, research method, editing and revising of the manuscript.

Funding

This work has been funded by CONAHCYT: the program: Estancia Posdoctoral Académica Inicial 2022(1) [Grant number 2466286, 487049].

Abbreviations

A_c	Collector area 2.506 (m^2)
A_s	Plate area (m^2)
C_1	Ca^{2+} concentration(kg/m^3),
C_2	CO_3^{2-} concentration(kg/m^3)
C_b	Thermal resistance between tube and plate (m^2 °C/W)
$Cost_a$	Annualised cost of solar collector ($/year)

ISSN: 2524-2121.
RENIECYT-CONAHCYT: 1702902

Lugo-Granados, Hebert Gerardo, Canizalez-Dávalos, Lázaro and Picón-Núñez, Martín. [2024]. Thermoeconomic analysis in solar collector fields: a focus on constant flowrate and variable flowrate models. ECORFAN-Journal Taiwan. 8 [15]1-12: e2815112.
https://doi.org/10.35429/EJT.2024.8.15.1.12

$Cost_b$	Operating cost ($)
$Cost_T$	Total operating cost ($)
$cost_u$	Unit cost of electricity ($/kwh)
Cp	Water heat capacity (kJ/kg °C)
C_u	Commercial cost of a solar collector ($811.76 dollars)
d_0	Collector tube outer diameter (m).
d_i	Collector tube inner diameter (m)
d_s	Hydraulic diameter (m)
f	Friction factor
$F´$	Collector efficiency factor
F_A	Metal fin thermal efficiency
Ƒa	Annualization factor
F_R	Heat removal factor
$ï$	Interest rate (8%)
I_G	Solar radiation (W/m^2)
K_1	Friction resistance (kPa s^2/m^6)
K_2	Hydraulic resistance due to connections (kPa s^2/m^6)
k_b	Thermal conductivity (W/m °C)
k_r	Reaction constant (m^2/kg s)
k_f	Resistance factor
K_s	Thermal conductivity of plate (W/m °C)
K_{sp}	$CaCO_3$ solubility (kg^2/m^6)
L_t	Tube length (m)
n	Collector lifespan.
m	Mass deposited in the storage tank each cycle (kg)
mT	Total mass deposited in the storage tank (kg)
$\dot{m}_d$	Mass flux (kg/m^2 s)
$\dot{m}_f$	Mass flow rate (kg/s)
$\dot{m}_r$	Mass flux removed (kg/m^2 s
Nc	Total number of collectors
Q	Process thermal load
Q_u	Useful heat (kW)
Q_T	Total heat load (kW)
Re	Reynolds number
R_h	Thermal resistance due to convection (m^2 °C/W)
R_s	Thermal resistance due to fouling (m^2 °C/W)
R_t	Thermal resistance due to conduction (m2 °C/W),
S	Distance between tubes (m)|
t	Operating time (h).
T_0	Outlet temperature (°C)
T_a	Ambient temperature (°C)
T_i	Inlet temperature (°C)
T_{tank}	Storage tank temperature
T_{pm}	Plate temperature (°C)
U_c	Overall heat transfer coefficient of losses (W/m^2°C)
W	Width (m)
x_f	Fouling layer thickness (m)
$\dot{V}$	Volumetric flow rate (m^3/s)
ΔP	Pressure drop (kPa)
$\dot{w}$	Pumping power

Symbols

α	Deposition resistance factor
α_c	Plate absorbance
β	Mass transfer coefficient (m/s)
γ	Thickness between plate and tube (m)
δ	Plate thickness (m)
εc	Boiler efficiency
η	Collector thermal efficiency
η_b	Pump efficiency
Θ	Cycle iteration
ï	Annual interest rate
λf	Thermal conductivity of $CaCO_3$ (W/m °C)
ρ	Density of water (kg/m^3)
ρf	Density of $CaCO_3$ (kg/m^3)
τ	Cover transmittance
ω	Collector lifespan of 20 years

References

Antecedents

Bunea, M., Eicher, S., Hildbrand, C., Bony, J., Perers, B., Citherlet, S. (2012). Performance of solar collectors under low temperature conditions: Measurements and simulations results. Eurosun, 1-8.

Hanson, M. L., Wendorff, W. L., Houck, K. B. (2005). Effect of Heat Treatment of Milk on Activation of Bacillus Spores. Journal of Food Protection, 1484–1486.

Basics

Dembeck-Kerekes, T., Fine J. P., Friedman J., Dworkin S. B., McArthur J. J. (2019). Performance of Variable Flow Rates for Photovoltaic Thermal Collectors and the Determination of Optimal Flow Rates. Solar Energy, 148-160.

Maroto-Izquierdo, B., Soria Verdugo, A. (2010). P asteurización de leche con Energía solar térmica. Universidad Carlos III de Madrid.

Sokhansefat, T., Kasaeian, A., Rahmani, K., Heidari, A. H, Aghakhani F., Mahian, O. (2018). Thermoeconomic and environmental analysis of solar flat plate and evacuated tube collectors in cold climatic conditions. Renewable Energy, 501-508.

ISSN: 2524-2121.
RENIECYT-CONAHCYT: 1702902

Lugo-Granados, Hebert Gerardo, Canizalez-Dávalos, Lázaro and Picón-Núñez, Martín. [2024]. Thermoeconomic analysis in solar collector fields: a focus on constant flowrate and variable flowrate models. ECORFAN-Journal Taiwan. 8 [15]1-12: e2815112.
https://doi.org/10.35429/EJT.2024.8.15.1.12

Zhuang, Z., Liu, Y., Chen Y., Zhao Y., Wang D., Ma J., Nan, S., (2024). An innovative variable flow control strategy and system performance analysis of a solar collector field. Applied Thermal Engineering, 123753.

Supports

Arunachala, U. C., Bhatt, M. S., Sreepathi, L. K. (2015). Analytical and Experimental Investigation to Determine the Variation of Hottel–Whillier–Bliss Constants for a Scaled Forced Circulation Flat-Plate Solar Water Heater. Sol. Energy Eng, 051011.

Du, B., Lund, P.D., Wang, J. (2022). Improving the accuracy of predicting the performance of solar collectors through clustering analysis with artificial neural network models. Energy Reports, 3970–3981.

Lugo-Granados, H., Picón Núñez M. (2018). Modelling scaling growth in heat transfer surfaces and its application on the design of heat exchangers. Energy, 845-854.

Lugo-Granados, H., Canizalez-Dávalos, L., Picón-Núñez, M. (2023). Thermohydraulic Effects of Scaling in Flat Plate Solar Collector Networks. Chemical Engineering Transactions, 421-426.

Lugo-Granados, H., Canizalez-Dávalos, L., Picón-Núñez, M. (2024). Flat plate solar collector networks: Design and retrofit considering fouling effects. Thermal Science and Engineering Progress, 102633.

Majumdar, R., Sahab, S. K., Patki, A. (2020). Novel dimension scaling for optimal mass flow rate estimation in low temperature flat plate solar collector based on thermal performance parameters. Thermal Science and Engineering Progress, 100569.

Momodu-Bangura, A. B., Hantoro, R., Fudhloli, A., Uwitije, P.D. (2022). Mathematical Model of the Thermal Performance of Double-Pass Solar Collector for Solar Energy Application in Sierra Leone. International Journal of Renewable Energy Development, 347-355.

Quan Z. H., Chen Y. C., Ma C. F. (2008). Heat mass transfer model of fouling process of calcium carbonate on heat transfer surface. Science in China Series Technological Sciences, 882-889.

Unterberger, V., Lichtenegger, K., Kaisermayer, V., Gölles, M., Horn, M. (2021). An adaptive short-term forecasting method for the energy yield of flat-plate solar collector systems. Applied. Energy, 116891.

Wang, D., Zhang, R., Liu, Y., Zhang, X., Fan, J. (2021). Optimization of the flow resistance characteristics of the direct return flat plate solar collector field. Solar Energy. 388–402.

ISSN: 2524-2121.
RENIECYT-CONAHCYT: 1702902

Lugo-Granados, Hebert Gerardo, Canizalez-Dávalos, Lázaro and Picón-Núñez, Martín. [2024]. Thermoeconomic analysis in solar collector fields: a focus on constant flowrate and variable flowrate models. ECORFAN-Journal Taiwan. 8 [15]1-12: e2815112.
https://doi.org/10.35429/EJT.2024.8.15.1.12